

*Supplement of*

## **Clumped-isotope-derived climate trends leading up to the end-Cretaceous mass extinction in northwest Europe**

**Heidi E. O’Hora et al.**

*Correspondence to:* Heidi E. O’Hora (ohora@umich.edu)

### **Contents:**

- **Figure S1:** oxygen isotope values of shell specimens and bulk carbonate;
- **Figure S2:** carbon isotope values of shell specimens and bulk carbonate;
- **Figure S3:** all  $\Delta_{47}$ -derived paleotemperature data, including samples removed due to diagenesis;
- **Table S1:** average paleotemperature data for all Maastrichtian-aged studies reconstructing marine temperatures used to create Figure 6;
- **Table S2:** all data for all samples including SEM results, trace elements, stable and clumped isotopes, paleotemperatures, and  $\delta^{18}\text{O}$  of seawater.

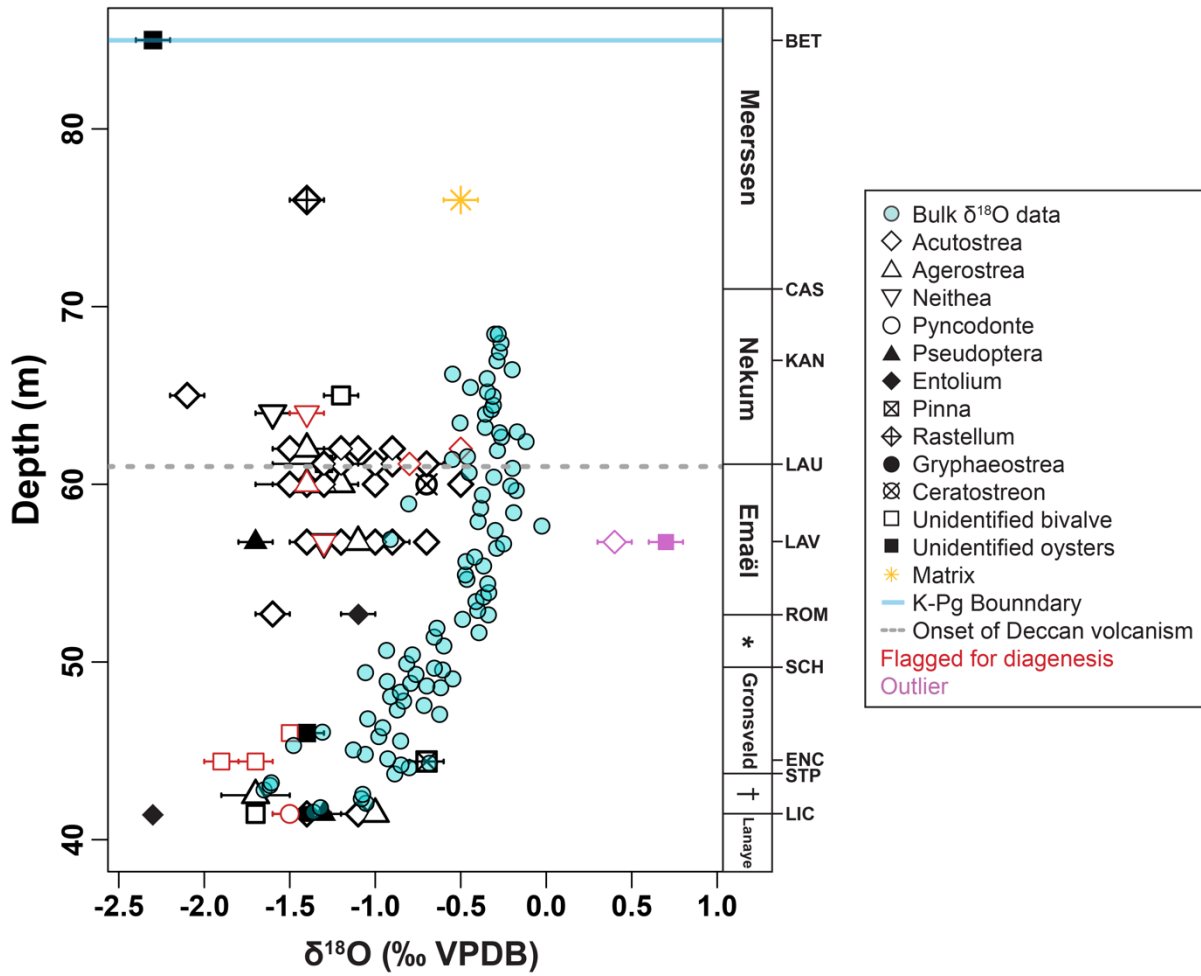


**Figure S1: Oxygen isotope values of shell specimens and bulk carbonate.** Bulk carbonate  $\delta^{18}\text{O}$  data from ENCI quarry are from Vellekoop et al. (in prep.). Red data points (flagged for diagenesis by trace element and/or SEM analysis) and purple points (outliers) were excluded from interpretation. If no error bars are visible, the uncertainty is smaller than the size of the symbol. Onset of the main Deccan Traps eruptions (grey dotted line) at 66.413 Ma (Sprain et al., 2019). K-Pg boundary (blue line) at 66.0 Ma. Member names and horizon abbreviations are labeled along right side of figure. Lanaye Member is part of underlying Gulpen Formation. \*Schiepersberg Member; †Valkenberg Member.

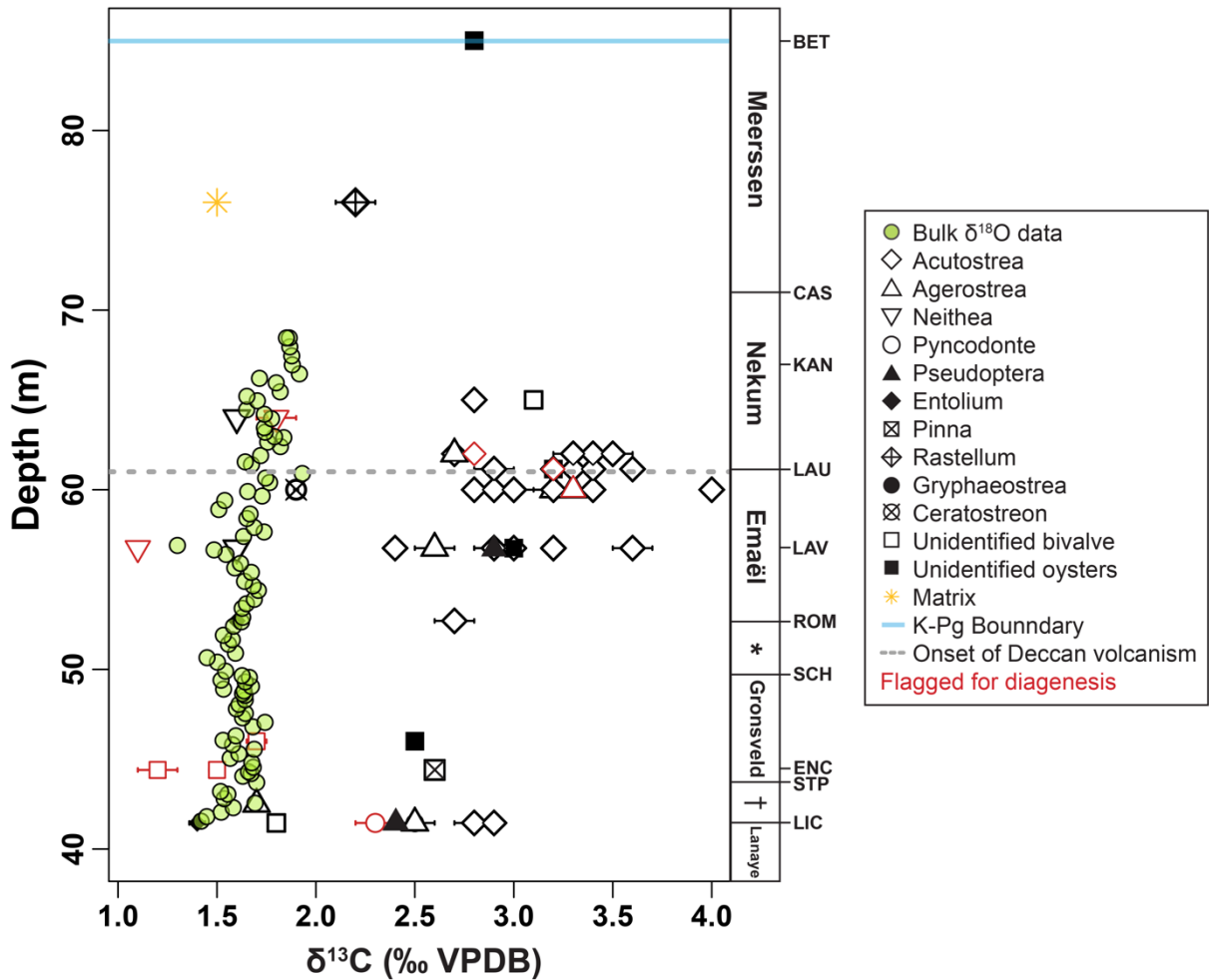


**Figure S2: Carbon isotope values of shell specimens and bulk carbonate.** Bulk carbonate  $\delta^{13}\text{C}$  data from ENCI quarry are from Vellekoop et al. (in prep.). Red data points (flagged for diagenesis by trace element and/or SEM analysis) were excluded from interpretation. If no error bars are visible, the uncertainty is smaller than the size of the symbol. Onset of the main Deccan Traps eruptions (grey dotted line) at 66.413 Ma (Sprain et al., 2019). K-Pg boundary (blue line) at 66.0 Ma. Member names and horizon abbreviations are labeled along right side of figure. Lanaye Member is part of underlying Gulpen Formation. \*Schiepersberg Member; †Valkenberg Member.

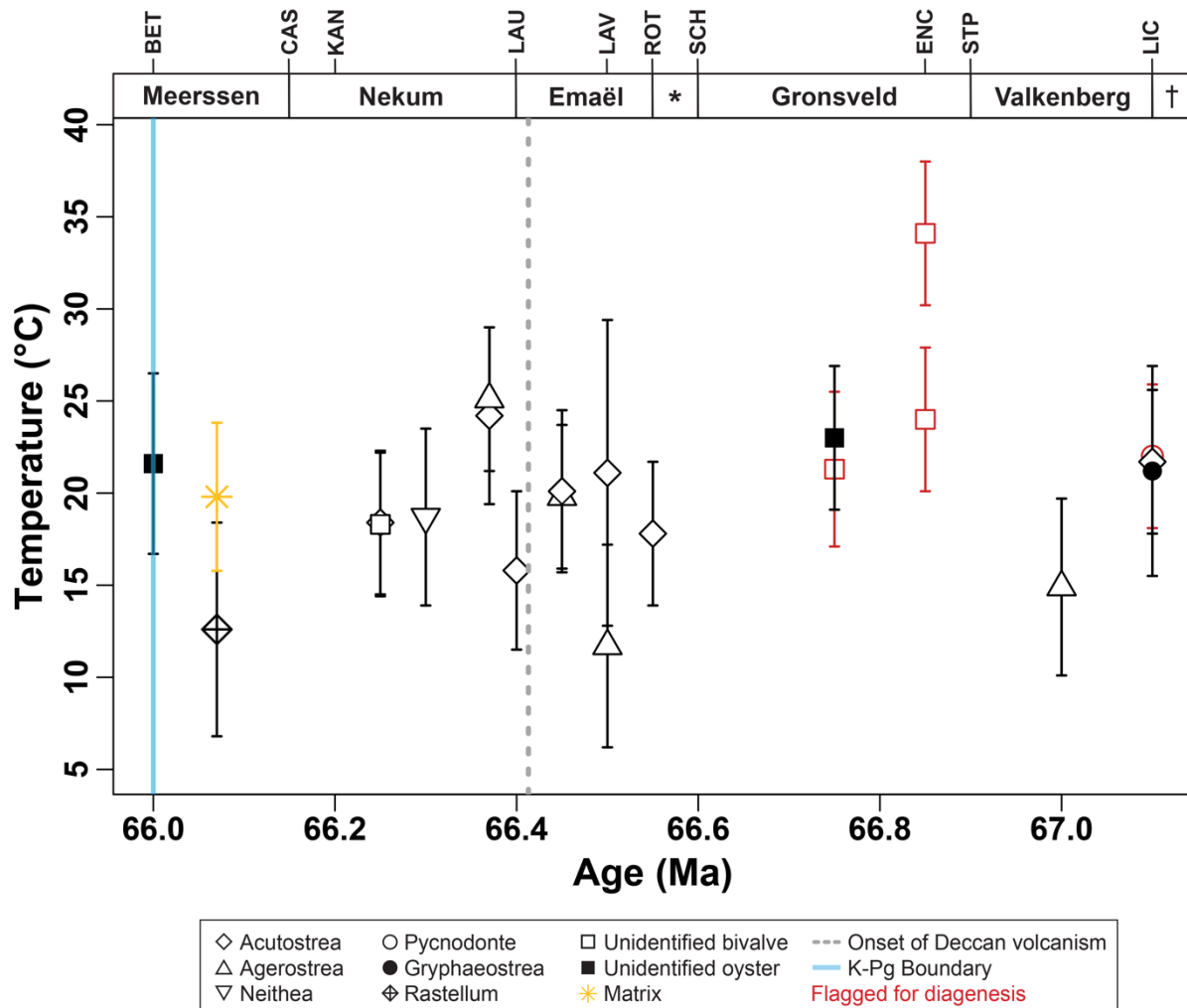


**Figure S3: All  $\Delta_{47}$ -derived paleotemperature data, including samples removed due to diagenesis.** Red data points (flagged for diagenesis by trace element and/or SEM analysis) were excluded from interpretation. Both internal and external standard error were calculated for all data points, and the larger of the two errors for each point is depicted here as an error bar. Onset of the main Deccan Traps eruptions (grey dotted line) at 66.413 Ma (Sprain et al., 2019). K-Pg boundary (blue line) at 66.0 Ma. Member names and horizon abbreviations are labeled across the top of the figure. \*Schiepersberg Member; †Lanaye Member (of underlying Gulpen Formation).

**Table S1: Average paleotemperature data for all Maastrichtian-aged studies reconstructing marine temperatures used to create Figure 6.** Data from this study is highlighted in red. All paleolatitudes were determined either directly from each study (if given) or via [www.paleolatitude.org](http://www.paleolatitude.org) (van Hinsbergen et al., 2015).

Study	Proxy type	Locality	Approx. age	Paleolat.	Avg. temp. (°C)
Meyer et al. (2019)	Clumped isotopes of clam, bivalve	North Slope, AK, USA	69.4 Ma	83	7.4
Dennis et al. (2013)	Clumped isotopes of gastropods, nautiloid, ammonites, belemnite, clams	Hell Creek, MT, USA	67.0–73.5 Ma	53	20.5
Tobin et al. (2014)	Clumped isotopes of gastropods, bivalves	Hell Creek, MT, USA	65.2–67.1 Ma	53	25.9
Zhang et al. (2018)	Clumped isotopes of paleosol carbonates	Songliao Basin, China	65.0–76.0 Ma	52	17.0
Meyer et al. (2019)	Clumped isotopes of belemnites, bivalves	Scania, Sweden	69.2–72.3 Ma	46	13.9
Tagliavento et al. (2019)	Clumped isotopes of coccolithic chalk	Danish Basin, Denmark	Late Campanian to Maastrichtian	46	24.5
Maestas et al. (2003)	Planktic foraminiferal $\delta^{18}\text{O}$	San Antonio Del Mar, Baja California	Late Campanian to Maastrichtian	42	19.5
Pucéat et al. (2007)	Phosphate $\delta^{18}\text{O}$ of fish teeth	Nasilov, Poland	66.0 Ma	40	14.6
Pucéat et al. (2007)	Phosphate $\delta^{18}\text{O}$ of fish teeth	South-Central NJ, USA	Mid to late Maastrichtian	40	14.4
This study	Clumped isotopes of oysters, clams, scallops	SE Netherlands & NE Belgium	66.0–67.4 Ma	40	19.2
Vellekoop et al. (2016)	TEX <sub>86</sub>	Monmouth County, NJ, USA	65.6–66.8 Ma	37	26.1
Meyer et al. (2018)	Clumped isotopes of oysters	Monmouth County, NJ, USA	70.7 Ma	37	13.8
Esmeray-Senlet et al. (2015)	Planktic foraminiferal $\delta^{18}\text{O}$	Bass River, NJ, USA	66.1–66.6 Ma	36	21.7
Woelders et al. (2018)	Planktic foraminiferal $\delta^{18}\text{O}$	Bass River, NJ, USA	66.0–66.3 Ma	36	25.2
Woelders et al. (2018)	TEX <sub>86</sub>	Bass River, NJ, USA	66.1–66.5 Ma	36	27.8
Woelders et al. (2018)	Planktic foraminiferal Mg/Ca	Bass River, NJ, USA	66.1–66.4 Ma	36	22.0
Meyer et al. (2018)	Clumped isotopes of oysters, clams, gastropod	Western TN, USA	73.5 Ma	36	21.5
Vellekoop et al. (2014)	TEX <sub>86</sub>	Brazos River, TX, USA	65.7–66.3 Ma	35	29.8
Meyer et al. (2018)	Clumped isotopes of oysters, clams	Moscow Landing, AL, USA	65.0–74.0 Ma	33	22.1
Meyer et al. (2018)	Clumped isotopes of oysters, clams, belemnite	Burches Ferry, SC, USA	71.4 Ma	33	20.6
Huber et al. (1995)	Planktic foraminiferal $\delta^{18}\text{O}$	Blake Nose, North Atlantic Ocean	Maastrichtian	31	18.6
Berggren and Norris (1997)	Planktic foraminiferal $\delta^{18}\text{O}$	DSDP 384, North Atlantic Ocean	64.9–66.2 Ma	31	9.8

Frank and Arthur (1999)	Planktic foraminiferal $\delta^{18}\text{O}$	Blake Nose, North Atlantic Ocean	Maastrichtian	31	21.1
Huber et al. (2002)	Planktic foraminiferal $\delta^{18}\text{O}$	Blake Nose, North Atlantic Ocean	66.0 Ma	31	18.1
Friedrich et al. (2004)	Planktic foraminiferal $\delta^{18}\text{O}$	Blake Nose, North Atlantic Ocean	69.6–71.3 Ma	31	19.6
MacLeod et al. (2005)	Planktic foraminiferal $\delta^{18}\text{O}$	Blake Nose, North Atlantic Ocean	Late Maastrichtian	31	21.4
Zakharov et al. (2006)	Planktic foraminiferal $\delta^{18}\text{O}$	Blake Nose, North Atlantic Ocean	Maastrichtian	31	18.3
Hull et al. (2020)	Bulk carbonate $\delta^{18}\text{O}$	IODP U1403, North Atlantic Ocean	66.0–68.8 Ma	31	11.2
Pucéat et al. (2007)	Phosphate $\delta^{18}\text{O}$ of fish teeth	Central Morocco	Maastrichtian	21	23.8
MacLeod et al. (2018)	Phosphate $\delta^{18}\text{O}$ of teeth	El Kef, Tunisia	65.8–66.4 Ma	21	22.6
Meyer et al. (2019)	Clumped isotopes of oysters, clams	Merced County, CA, USA	69.7–78.0 Ma	21	16.5
Hull et al. (2020)	Bulk and planktic foraminiferal $\delta^{18}\text{O}$	ODP 1209, North-West Pacific Ocean	65.8–66.0 Ma	21	18.2
Hull et al. (2020)	Bulk carbonate $\delta^{18}\text{O}$	ODP 1209, North-West Pacific Ocean	64.1–66.1 Ma	21	12.4
Meyer et al. (2019)	Clumped isotopes of oysters	Fezzan region, Libya	70.9–71.4 Ma	11	29.2
Li and Keller (1998)	Planktic foraminiferal $\delta^{18}\text{O}$	DSDP 525, South Atlantic Ocean	66.0–66.5 Ma	-40	15.0
Kroon et al. (2007)	Bulk carbonate $\delta^{18}\text{O}$	ODP 1262, South Atlantic Ocean	65.0–67.1 Ma	-41	9.9
Birch et al. (2016)	Planktic foraminiferal $\delta^{18}\text{O}$	ODP 1262, South Atlantic Ocean	66.0–66.5 Ma	-41	14.5
Woelders et al. (2017)	TEX <sub>86</sub>	Bajada del Jagüel, Argentina	64.0–66.7 Ma	-43	27.2
Tobin et al. (2012)	$\delta^{18}\text{O}$ of bivalves, gastropods	Seymour Island, Antarctica	65.7–68.5 Ma	-65	8.1
Petersen et al. (2016a)	Clumped isotopes of clams, cockles	Seymour Island, Antarctica	65.8–69.0 Ma	-65	7.7
Stott and Kennett (1990)	Planktic foraminiferal $\delta^{18}\text{O}$	ODP 690, South Atlantic Ocean	65.5–68.4 Ma	-70	10.6
Wilf et al. (2003)	Planktic foraminiferal $\delta^{18}\text{O}$	ODP 690, South Atlantic Ocean	66.1–66.5 Ma	-70	10.6

**Table S2: All data for all samples including SEM results, trace elements, stable and clumped isotopes, paleotemperatures, and  $\delta^{18}\text{O}$  of seawater.** Red samples were excluded from interpretation due to elevated trace element concentrations and/or SEM analysis. Purple samples were excluded from interpretation due to anomalously high  $\delta^{18}\text{O}$  values. The yellow data are from the matrix sample. In the SEM column, SG means secondary growth and diss means dissolution.

Sample ID	Site	Strat	Depth (m)	Age (Ma)	Taxa	SEM	Mg (ppm)	Fe (ppm)	$\delta^{18}\text{O}$ (%VPDB)	$\delta^{18}\text{O}$ STD	$\delta^{13}\text{C}$ (%VPDB)	$\delta^{13}\text{C}$ STD	$\Delta_{47}$ (%VPDB)	$\Delta_{47}$ error	Temp (°C)	Temp error	$\delta^{18}\text{O}_{\text{sw}}$ (%VSMOW)	$\delta^{18}\text{O}_{\text{sw}}$ error	
LIC-Psop	ENCI, NL	Lichtenberg Hz	41.45	67.1	psop	NA	1779.67	68.9	1008.85	-1.3	0.04	2.4	0.02	NA	NA	NA	NA	NA	NA
LIC-Pycn	ENCI, NL	Lichtenberg Hz	41.45	67.1	pycn	SG	4027.37	85.9	4441.3	-1.5	0.1	2.3	0.1	0.698	0.013	22.0	3.9	0.2	0.9
LIC-AcutA	ENCI, NL	Lichtenberg Hz	41.45	67.1	acut	NA	1616.95	37.1	1718.3	-1.4	0.1	2.8	0.1	0.699	0.013	21.7	3.9	0.3	0.9
LIC-Gry	ENCI, NL	Lichtenberg Hz	41.45	67.1	gry	NA	1412.07	41.8	881.5	-1.4	0.2	2.5	0.1	0.701	0.017	21.2	5.7	0.2	1.2
LIC-AcutB	ENCI, NL	Lichtenberg Hz	41.45	67.1	acut	NA	1517.77	44.4	227.93	-1.1	0.1	2.9	0.03	NA	NA	NA	NA	NA	NA
LIC-Ager	ENCI, NL	Lichtenberg Hz	41.45	67.1	ager	NA	1693.07	59.14	390.33	-1.0	0.02	2.5	0.01	NA	NA	NA	NA	NA	NA
LIC-Biv	ENCI, NL	Lichtenberg Hz	41.45	67.1	biv	NA	3539.90	89.22	217.45	-1.7	0.04	1.8	0.01	NA	NA	NA	NA	NA	NA
LIC-Ento	ENCI, NL	Lichtenberg Hz	41.45	67.1	ento	NA	2676.27	88.39	645.54	-2.3	0.01	1.4	0.04	NA	NA	NA	NA	NA	NA
VAL-Ager	ENCI, NL	Valkenberg Mem	42.5	67.0	ager	NA	2615.75	89.1	1101.6	-1.7	0.2	1.7	0.03	0.720	0.016	14.9	4.8	-1.4	1.1
ENC-Pinna	ENCI, NL	ENCI Hz	44.4	66.85	pinna	NA	3783.09	22.8	475.2	-0.7	0.1	2.6	0.03	NA	NA	NA	NA	NA	NA
ENC-BivA	ENCI, NL	ENCI Hz	44.4	66.85	biv	NA	4955.74	105.5	4345.3	-1.7	0.1	1.5	0.04	0.692	0.013	24.0	3.9	0.5	0.9
ENC-BivB	ENCI, NL	ENCI Hz	44.4	66.85	biv	diss/SG	4708.41	128	3354.7	-1.9	0.1	1.2	0.1	0.664	0.013	34.1	3.9	2.3	0.9
GRO-Biv	ENCI, NL	Gronsveld Mem	46	66.75	biv	NA	3162.58	210.3	713.0	-1.5	0.02	1.7	0.05	0.700	0.013	21.3	4.2	0.1	0.9
GRO-Ost	ENCI, NL	Gronsveld Mem	46	66.75	oyst	NA	1379.27	55.2	370.5	-1.4	0.1	2.5	0.02	0.695	0.013	23.0	3.9	0.6	0.9
ROT-Acut	ENCI, NL	Romontbos Hz	52.7	66.55	acut	NA	2374.14	50.4	295.1	-1.6	0.1	2.7	0.1	0.710	0.013	17.8	3.9	-0.7	0.9
ROT-Ento	ENCI, NL	Romontbos Hz	52.7	66.55	ento	NA	4576.72	72.7	1032.1	-1.1	0.1	1.6	0.03	NA	NA	NA	NA	NA	NA
LAV-AcutG	ENCI, NL	Lava Hz	56.75	66.5	acut	NA	1750.24	29.6	597.5	-1.4	0.1	3.2	0.03	NA	NA	NA	NA	NA	NA
LAV-NeitA	ENCI, NL	Lava Hz	56.75	66.5	neit	NA	2404.16	66.5	3201.1	-1.3	0.1	1.1	0.03	NA	NA	NA	NA	NA	NA
LAV-NeitB	ENCI, NL	Lava Hz	56.75	66.5	neit	original	2263.15	41.89	7114.8	-1.3	0.02	1.6	0.01	NA	NA	NA	NA	NA	NA
LAV-AcutA	ENCI, NL	Lava Hz	56.75	66.5	acut	NA	3323.55	69.3	1084.3	-0.9	0.1	2.9	0.1	0.704	0.025	21.1	8.3	0.6	1.7
LAV-AcutB	ENCI, NL	Lava Hz	56.75	66.5	acut	original	3073.97	58.8	285.8	-0.7	0.03	3.0	0.02	NA	NA	NA	NA	NA	NA
LAV-AcutC	ENCI, NL	Lava Hz	56.75	66.5	acut	NA	964.16	23.6	594.9	-1.2	0.1	3.2	0.02	NA	NA	NA	NA	NA	NA
LAV-AcutD	ENCI, NL	Lava Hz	56.75	66.5	acut	NA	1978.87	60.91	636.42	-1.2	0.04	2.9	0.02	NA	NA	NA	NA	NA	NA
LAV-AcutE	ENCI, NL	Lava Hz	56.75	66.5	acut	NA	2604.28	47.7	688.9	0.4	0.1	3.6	0.1	NA	NA	NA	NA	NA	NA
LAV-AcutF	ENCI, NL	Lava Hz	56.75	66.5	acut	NA	3872.70	78.46	95.64	-1.0	0.04	2.4	0.03	NA	NA	NA	NA	NA	NA
LAV-Ost	ENCI, NL	Lava Hz	56.75	66.5	oyst	NA	3365.03	75.81	599.37	-0.7	0.1	3.0	0.04	NA	NA	NA	NA	NA	NA
LAV-Ager	ENCI, NL	Lava Hz	56.75	66.5	ager	NA	2123.12	49.1	1561.4	-1.1	0.2	2.6	0.1	0.732	0.019	11.7	5.5	-1.6	1.3
LAV-Psop	ENCI, NL	Lava Hz	56.75	66.5	psop	NA	1663.84	48.03	268.6	-1.7	0.1	2.9	0.1	NA	NA	NA	NA	NA	NA
EMAU-AgerA	ENCI, NL	Emael Mem	60	66.45	ager	NA	1034.35	36.01	376.01	-1.2	0.04	3.3	0.04	NA	NA	NA	NA	NA	NA
EMAU-AgerB	ENCI, NL	Emael Mem	60	66.45	ager	diss/SG	1844.76	40.16	578.15	-1.4	0.1	3.3	0.1	NA	NA	NA	NA	NA	NA
EMAU-AgerC	ENCI, NL	Emael Mem	60	66.45	ager	NA	1156.41	40.4	2013.3	-1.4	0.3	3.2	0.2	0.704	0.013	19.8	3.9	-0.1	0.9
EMAU-AcutA	ENCI, NL	Emael Mem	60	66.45	acut	NA	1032.29	35.1	NA	-1.5	0.1	3.2	0.1	0.704	0.014	20.1	4.4	-0.1	1.0
EMAU-AcutC	ENCI, NL	Emael Mem	60	66.45	acut	diss	2194.64	60.1	2422.7	-1.0	0.04	2.8	0.02	NA	NA	NA	NA	NA	NA
EMAU-AcutD	ENCI, NL	Emael Mem	60	66.45	ager	NA	1195.54	34.84	102.81	-1.4	0.1	2.9	0.01	NA	NA	NA	NA	NA	NA
EMAU-AcutE	ENCI, NL	Emael Mem	60	66.45	acut	NA	1880.18	28.4	347.7	-1.3	0.1	3.0	0.04	NA	NA	NA	NA	NA	NA
EMAU-AcutF	ENCI, NL	Emael Mem	60	66.45	acut	original	2384.95	58.15	1141.76	-0.5	0.01	3.4	0.01	NA	NA	NA	NA	NA	NA
EMAU-AgerD	ENCI, NL	Emael Mem	60	66.45	ager	NA	1815.13	27.87	175.96	-1.3	0.01	3.3	0.01	NA	NA	NA	NA	NA	NA
EMAU-AcutG	ENCI, NL	Emael Mem	60	66.45	acut	original	1556.77	37.1	1514.5	-1.5	0.03	3.0	0.02	NA	NA	NA	NA	NA	NA
EMAU-AcutH	ENCI, NL	Emael Mem	60	66.45	acer	NA	2127.29	19.23	261.69	-1.3	0.03	4.0	0.01	NA	NA	NA	NA	NA	NA
EMAU-Cer	ENCI, NL	Emael Mem	60	66.45	cer	NA	1745.09	35.3	511.9	-0.7	0.01	1.9	0.01	NA	NA	NA	NA	NA	NA
LAU-Unoy	ENCI, NL	Laumont Hz	61.15	66.4	oyst	diss	1953.30	57.04	7114.3	-1.3	0.02	3.2	0.02	NA	NA	NA	NA	NA	NA
LAU-AcutA	ENCI, NL	Laumont Hz	61.15	66.4	acut	NA	2603.99	99.8	7151.1	-0.8	0.1	3.2	0.04	NA	NA	NA	NA	NA	NA
LAU-AcutB	ENCI, NL	Laumont Hz	61.15	66.4	acut	NA	1947.88	41.91	268.89	-1.3	0.03	3.2	0.02	NA	NA	NA	NA	NA	NA
LAU-AcutC	ENCI, NL	Laumont Hz	61.15	66.4	acut	NA	867.99	37.9	2007.8	-1.2	0.02	3.2	0.01	NA	NA	NA	NA	NA	NA
LAU-AcutD	ENCI, NL	Laumont Hz	61.15	66.4	acut	NA	1118.03	47.6	1907.1	-1.0	0.1	3.3	0.01	NA	NA	NA	NA	NA	NA
LAU-AcutE	ENCI, NL	Laumont Hz	61.15	66.4	acut	original	1222.74	38.55	166.09	-0.7	0.1	3.4	0.04	NA	NA	NA	NA	NA	NA
LAU-AcutF	ENCI, NL	Laumont Hz	61.15	66.4	acut	NA	727.62	48.6	1014.2	-1.3	0.3	2.9	0.1	0.717	0.014	15.8	4.3	-0.9	1.1
LAU-AcutG	ENCI, NL	Laumont Hz	61.15	66.4	acut	diss	1483.89	36.2	1163.09	-0.9	0.1	3.6	0.02	NA	NA	NA	NA	NA	NA
NEKB-AcutA	ENCI, NL	Nekum Mem (base)	62	66.37	acut	NA	1169.96	24.6	724.2	-1.1	0.01	3.4	0.03	0.691	0.016	24.2	4.8	1.1	1.1
NEKB-AcutB	ENCI, NL	Nekum Mem (base)	62	66.37	acut	original	1769.21	35.95	248.56	-1.2	0.1	3.3	0.1	NA	NA	NA	NA	NA	NA
NEKB-AcutD	ENCI, NL	Nekum Mem (base)	62	66.37	acut	diss	1365.33	16.66	225.46	-1.5	0.1	3.5	0.1	NA	NA	NA	NA	NA	NA
NEKB-AcutE	ENCI, NL	Nekum Mem (base)	62	66.37	acut	diss	2481.96	41.9	2068.5	-0.9	0.03	2.7	0.04	NA	NA	NA	NA	NA	NA
NEKB-AcutF	ENCI, NL	Nekum Mem (base)	62	66.37	acut	NA	2174.63	46.2	3608.6	-0.5	0.02	2.8	0.01	NA	NA	NA	NA	NA	NA
NEKB-Ager	ENCI, NL	Nekum Mem (base)	62	66.37	ager	NA	1981.93	59.8	386.7	-1.4	0.1	2.7	0.03	0.689	0.013	25.1	3.9	1.0	0.9
NEK-Neit	ENCI, NL	Nekum Mem (mid)	64	66.3	neit	diss/SG	2677.14	45.53	435.62	-1.4	0.1	1.8	0.1	NA	NA	NA	NA	NA	NA
NEK-NeitB	ENCI, NL	Nekum Mem (mid)	64	66.3	neit	NA	2122.18	38.9	285.8	-1.6	0.1	1.6	0.04	0.708	0.016	18.7	4.8	-0.5	1.1
CBR-Acut	CBR, BE	Nekum Mem (CBR)	65	66.25	acut	NA	2361.67	31.1	482.2	-2.1	0.1	2.8	0.04	0.709	0.013	18.4	3.9	-1.1	0.9
CBR-Biv	CBR, BE	Nekum Mem (CBR)	65	66.25	biv	NA	2291.73	21.4	225.5	-1.2	0.1	3.1	0.03	0.709	0.013	18.3	3.9	-0.2	0.9
MEER-RasB	ENCI, NL	Meerssen Mem	76	66.07	ras	original	1194.89	34.8	843.0	-1.4	0.1	2.2	0.1	0.729	0.020	12.6	5.8	-1.7	1.3
MEER-Mat	ENCI, NL	Meerssen Mem	76	66.07	mat	NA	5989.04	60.2	607.1	-0.9	0.1	1.5	0.04	0.709	0.013	19.1	4.0	0.1	0.9
GCAV-OystA	GSGs, NL	Berg en Terblijt Hz	85	66.0	oyst	original	861.60	60.82	245.33	-2.3	0.1	2.8	0.01	0.699	0.013	21.6	4.9	-0.6	0.9